First-principles study of electronic structures, thermodynamic, and thermoelectric properties of the new Rattling Full Heusler compounds Ba2AgZ (Z = As, Sb, Bi)

Kalaliz Kheira, A. Chahed, M. A. Boukli, M. A. Khettir, A. Oughilas, Adlane Sayede

First-principles study of electronic structures, thermodynamic, and thermoelectric properties of the new rattling Full Heusler compounds Ba_2AgZ (Z = As, Sb, Bi)

K. Kalaliz[a,*], A. Chahed[a], M.A Boukli[a], M.A. Khettir[a], A. Oughilas[b], and A. Sayede[b]

[a] *Condensed Matter and Sustainable Development Laboratory, University of Sidi Bel-Abbes, Sidi Bel-Abbes 22000, Algeria.*

[*] *e-mail: kalalizkheira2@gmail.com*

[b] *UCCS, CNRS-UMR 8181, Université d'Artois, Faculté des Sciences Jean Perrin, Rue Jean Souvraz, SP 18, 62307 Lens Cedex, France.*

Received 7 March 2021; accepted 11 May 2021

The ab initio calculations based on the density functional theory (DFT) using the self-consistent Full potential linearized augmented plane wave (FPLAPW) method were performed to explore the electronic structures, thermodynamic and thermoelectric properties of new rattling Full Heusler alloys Ba_2AgZ (Z = As, Sb, Bi). Results showed that the $AlCu_2Mn$-type structure state is energetically the most stable structure. The results show that the electronic property of these cubic Rattling Heusler alloys has a semiconducting behavior with indirect band gaps E_g (L-Δ). The predicted band gaps were found to be 0.566, 0.548, and 0.433 eV for Z = As, Sb, and Bi, respectively. The thermodynamic properties comprising the thermal expansion coefficient, heat capacity, entropy and Debye temperature parameter were evaluated at various pressures from 0 to 15 GPa. Thermoelectric properties of the Ba_2AgZ (Z = As, Sb, Bi) materials are additionally computed over an extensive variety of temperatures, and it is discovered that all compounds exhibit ultralow thermal conductivity, good Seebeck coefficients, and large high power factors, thus resulting they are suitable for use in thermoelectric device applications.

Keywords: Heusler compounds; density functional theory; electronic structures; thermodynamic properties; thermoelectric properties.

PACS: 71.20.Nr; 71.15.Mb; 71.20.-b; 65.40.Gr; 74.25.Fy

DOI: https://doi.org/10.31349/RevMexFis.67.060501

1. Introduction

The search for clean and renewable energy is currently an urgent challenge globally. The utilization of waste heat has been gaining increasing attention with the increasingly serious problems of fossil energy depletion and environmental pollution. Thermoelectric materials have attracted increasing attention because they can harvest waste heat and convert it directly into electricity, given their promising performances in energy conversion applications. The conversion efficiency is measured by the dimensionless figure of merit $ZT = S^2\sigma T/(\kappa_e+\kappa_L)$, where T is the absolute temperature, S is the thermopower, σ is the electrical conductivity, and κ_e and κ_L are the electronic and lattice thermal conductivities, respectively. Optimizing ZT thus involves the tuning of conflicting material properties by maximizing the power factor (PF) $S^2\sigma$ and minimizing thermal conductivity (κ_e and κ_L) simultaneously.

Research on Heusler alloys, Half Heusler (HH) and Full Heusler (FH), having, respectively, a general formula XYZ and X_2YZ (X/Y are transition metals, $Z = p$-block elements) have constantly drawn the attention of the researchers due to their remarkable various applications, such as Half metals [1], ferromagnetic shape memory alloys [2], superconductivity [3], and spintronics [4]. Also, as for compounds HH compounds, the Full Heusler (FH) materials have thus attracted attention as thermoelectric (TE) materials [5-9]. Although very high PFs at room temperature have been reported in FH compounds based on Fe2VAl [10-12], the effective ZT values are merely around $0.13-0.2$ at 300 K due to the high thermal conductivity (intrinsic $\kappa_L = 28$ W·m^{-1}K^{-1}). Recently, Bilc *et al*. predicted several FH compounds through bielemental substitution in Fe_2YZ (Y = V, Nb, Ta, Ti, Zr, Hf ; Z = Al, Ga, Sn, Ge, Si), thereby demonstrating the possibility of boosting the PF by a factor of 5 through band engineering [13].

Nevertheless, the search for novel, highly efficient, and cost-effective materials is an open challenge to researchers; and in contrast to conventional FH compounds, there are a new class of stable semiconducting FH compounds with intrinsically high PFs and extremely low lattice thermal conductivity due to atomic rattling, which we call R. Heusler (Rattling Heusler) compounds. These compounds, which to our knowledge have very little been reported in the literature, contain ten valence electrons per f.u. [14-16]. In order to enlarge studies in this new field of material, we investigate in this paper the structural, electronic, thermodynamic, and thermoelectric properties of the three new Rattling Heuslers Ba_2AgZ (Z = As, Sb, Bi) with alkaline earth elements Ba in the X sublattice, whereas Ag is a noble metal and Z is As, Sb and Bi elements. It is expected that this paper will open new avenues for especially thermoelectric applications. The remainder of the article is organized as follows: The technical details of calculations have been reported in Sec. 2. The details of crystal structure and the main results for the structural,

electronic, thermodynamic, and thermoelectric properties are presented in Sec. 3. A brief conclusion of the results is finally given in Sec. 4.

2. Method of calculations

We have carried out first the principles calculations [17,18] with both Full potential and linear augmented plane wave (FP-LAPW) methods [19] as implemented in the WIEN2k code [20]. The exchange-correlation effects were described with the parameterization of the generalized gradient approximation (GGA) [21]. Well-converged basis sets are chosen with $R_{MT}\ K_{\max} = 8$ while $G_{\max} = 12Ry^{1/2}$ for the Fourier charge density expansion of the potential in the interstitial region is used. A mesh of 104 special k-points was made in the irreducible wedge of the Brillouin zone. An energy threshold of -6 Ry is used to separate the valance and core states for all calculations.

3. Results and discussions

3.1. Structural properties

As is known, the so-called Full Heusler alloys crystallize in a highly ordered cubic structure, and their properties are related to the site preference of the atoms inside the structure. There are two types of highly ordered atomic arrangements [22]: $AlCu_2Mn$ (space group 225 $F-m3m$) and $CuHg_2Ti$-type structures (space group 216 $F-43m$). For Ba_2AgZ (Z = As, Sb, Bi) alloys in the $AlCu_2Mn$-type structure, the atomic sites are described as follows in Wyckoff coordinates: Ba (0,0,0), Ba (0.5,0.5,0.5), Ag (0.25,0.25,0.25), and Z (0.75,0.75,0.75), and in the $CuHg_2Ti$-type structure, they are Ba (0,0,0), Ba (0.25,0.25,0.25), Ag (0.5,0.5,0.5), and Z (0.75,0.75,0.75). Structural optimizations on the Ba_2AgZ (Z = As, Sb, Bi) alloys were performed first to determine their equilibrium lattice constants. The total energy-lattice constant curves for these alloys are plotted in Fig. 1. Clearly, the $AlCu_2Mn$-type structure state is energetically the most stable structure in comparison to the Hg_2CuTi-type at the equilibrium lattice constant for these three alloys. The values of the optimized parameters are given in Table I and are 8.06, 8.35, and 8.46 A° for Ba_2AgAs, Ba_2AgSb and Ba_2AgBi, respectively. The equilibrium lattice constant of these alloys increases with the increasing covalent radii of the Z atoms (*i.e.*, As→Sb→Bi). The formation energy E_f determines whether a compound can be experimentally synthesized or not [23]. E_f is the change in energy when a material is formed from its constituent elements in its bulk states and can be calculated for Ba_2AgZ (Z = As, Sb, Bi) compounds as $E_f = (E_{tot} - 2E_{\mathrm{Ba}} - E_{\mathrm{Ag}} - E_{\mathrm{Z}})$ with Z = Al, Si, Ge, As. Table I shows that the values of all compounds are negative, which confirms that these compounds are stable and can be synthesized experimentally. Among them, Ba_2AgAs is most easily synthesized because of its lowest formation energy. Thus, in order to consolidate our predictive results of our Ba_2AgZ (Z = As, Sb, Bi) Full-Heusler alloys, we have compared ours results in Table I with the other theoretically work for the same family of rattling Heusler Ba_2AuZ (Z = Sb, Bi) alloys [15]. The obtained results stay in good agreement with this theoretical study. Based on this, all the further calculations on electronic, thermodynamic and thermoelectric properties of Ba_2AgZ (Z = As, Sb, Bi) were performed on in the type-Cu_2MnAl structure.

3.2. Electronic properties

It is well known that the band structure is vital for determining the thermoelectric properties because these properties depend greatly on the band structure. The calculated band structures of Ba_2AgZ (Z = As, Sb, Bi) R compounds have been illustrated in Figs. (2-4)a. As it can be seen, the general band structures of are similar for our R FH compounds. The va-

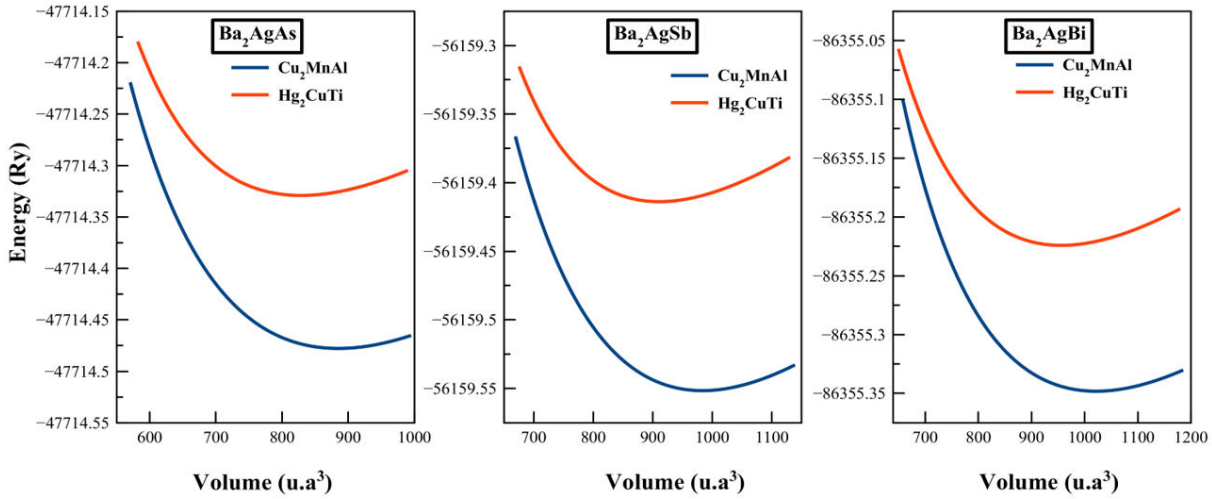

FIGURE 1. Total energy as a function of unit cell volume for the Ba_2AgZ (Z = As, Sb, Bi) compounds in both Cu_2MnAl and Hg_2CuTi type structure.

TABLE I. Calculated total energies E_{tot} (in Ry) per formula unit, equilibrium lattice constant a_0 (in Å), the bulk modulus B (in GPa), the formation energy (in Ry) and the energy gap $E_g(L-\Delta)$(in eV) for Ba_2AgZ (Z= As, Sb, Bi) compounds in theirs different structures type configurations.

Compound	structure	E_{tot}	a_0	B_0	E_f	$E_g(L-\Delta)$
Ba_2AgAs	Cu_2MnAl	-47714.477781	8.065	32.43	-0.84	0.566
	Hg_2CuTi	-47714.329083	7.890	30.77	-0.56	
Ba_2AgSb	Cu_2MnAl	-56159.551580	8.353	28.24	-0.748	0.548
	Hg_2CuTi	-56159.413848	8.143	26.38	-0.535	
Ba_2AgBi	Cu_2MnAl	-86355.348178	8.460	25.62	-0.52	0.433
	Hg_2CuTi	-86355.223962	8.273	24.09	-0.19	
Ba_2AuSb[15]$^{FP\text{-}LAPW}$	Cu_2MnAl		8.28	32		0.72
Ba_2AuBi[15]$^{FP\text{-}LAPW}$	Cu_2MnAl		8.37	30		0.57

lence band maximum (VBM) and conduction band minimum (CBM) are located at the low symmetry points L and Δ (between Γ and X) in the Brillouin zone indicate that Ba_2AgZ (Z = As, Sb, Bi) alloys are indirect bandgap semiconductors. The indirect energy gap E_g $(L-\Delta)$ of 0.566 eV for Ba_2AgAs, 0.548 eV Ba_2AgSb and 0.433 eV for Ba_2AgBi is obtained. Unfortunately, so far, no experimental measurements and theoretical data bandgap E_g for the investigated compounds are carried out to compare with. However, our results for bandgap E_g listed in Table I are in good agreement with the other theoretically work for the same family of rattling Full Heusler Ba_2AuZ (Z = Sb, Bi) [15].

Furthermore, multiple bands have energies close to the VBM and CBM and lead to a sharp increase in the density of states around the Fermi level, which is favorable for large Seebeck coefficients. Bilc *et al.* [13] recently showed that bands that are flat along one direction and highly dispersive along others lead to a high Power factor (PF) in FH materials. In fact, such bands are present in ours new R compounds Ba_2AgZ (Z = As, Sb, Bi) as well, where the valence band along $L-\Gamma$ is flat, whereas it is highly dispersive along with all other directions, as depicted in the red circle of band structures. The total (TDOS) and partial (PDOS) densities of states are plotted in Figs. (2-4)b for these three compounds.

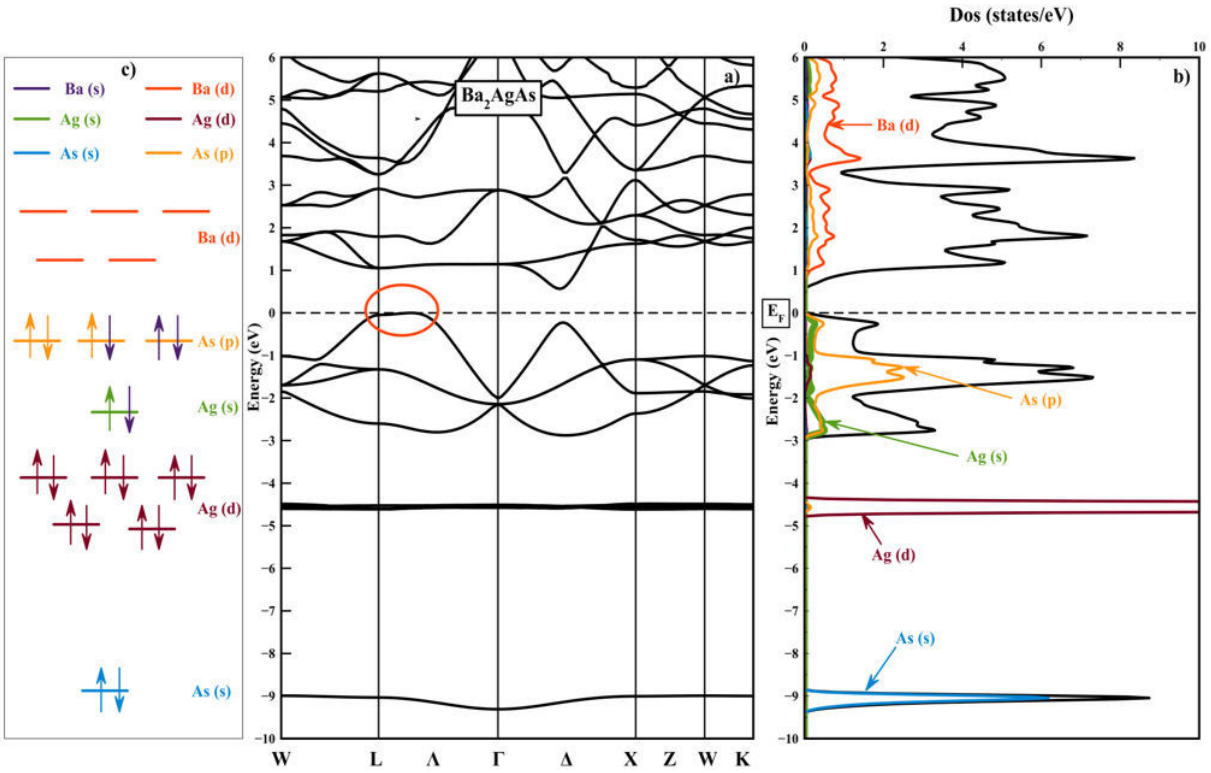

FIGURE 2. Band structure and total and partial density of states for the Ba_2AgAs compound.

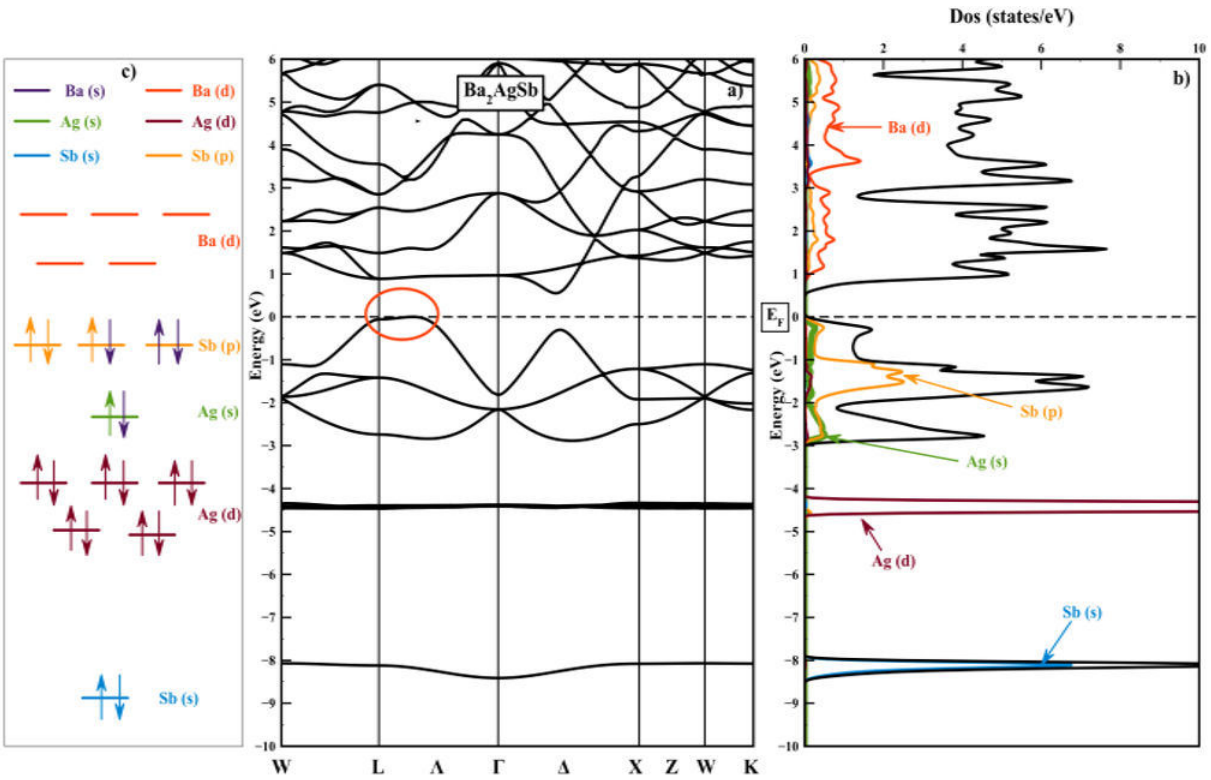

FIGURE 3. Band structure and total and partial density of states for the Ba_2AgSb compound.

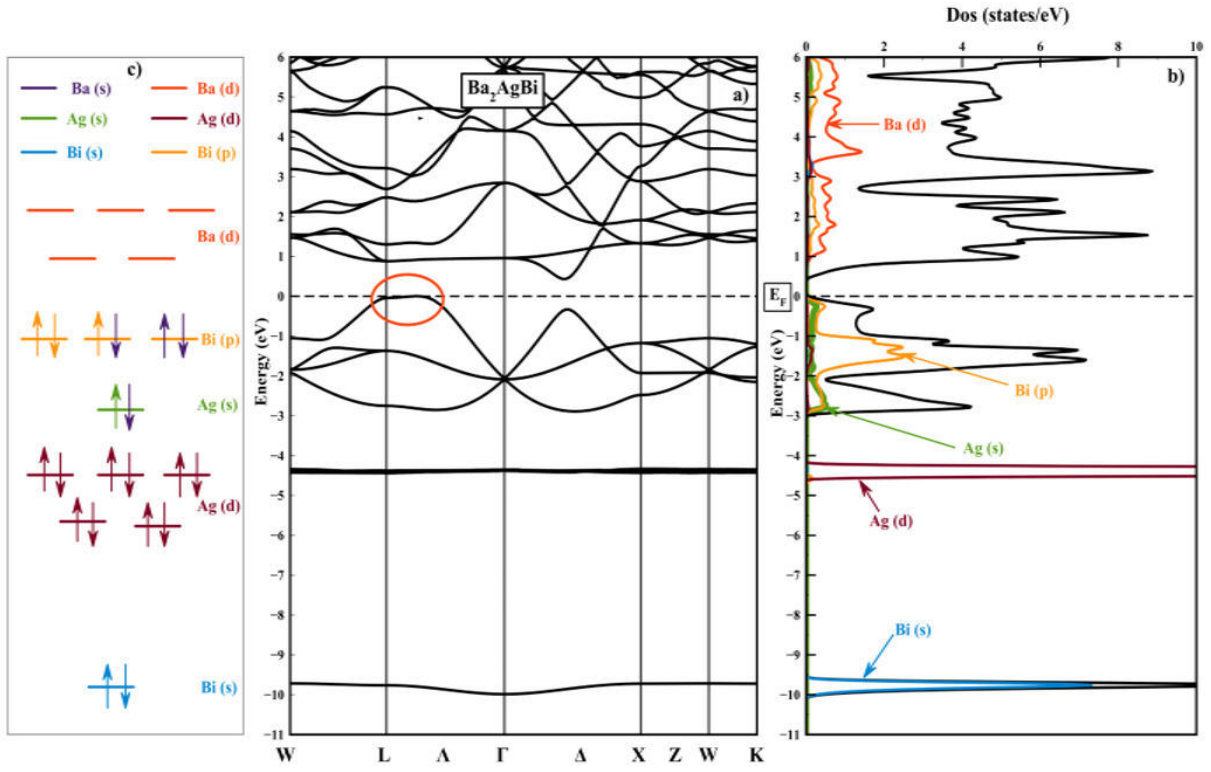

FIGURE 4. Band structure and total and partial density of states for the Ba_2AgBi compound.

TABLE II. Calculated elastic constants C_{ij} (in GPa), Bulk modulus B (in GPa), Poisson's ratio v, anisotropy factor A and B/G ratio for Ba_2AgZ (Z = As, Sb, Bi) compounds.

Compound	C_{11}	C_{12}	C_{44}	B	v	A	B/G
Ba_2AgAs	59.96	18.86	15.64	32.56	0.27	0.76	1.87
Ba_2AgSb	55.67	14.33	7.97	28.11	0.33	0.38	2.38
Ba_2AgBi	57.12	11.72	17.80	26.85	0.21	0.78	1.37

TABLE III. Calculated values of heat capacity C_V (in J·mol^{-1}·K^{-1}), entropy S (J·mol^{-1}·K^{-1}) and Debye temperature θ_D (in K) at 300 K for Ba_2AgZ (Z= As, Sb, Bi) compounds.

Compound	C_v	S	θ_D
Ba_2AgAs	98.08	185.35	175.55
Ba_2AgSb	98.35	195.68	161.26
Ba_2AgBi	98.56	203.73	148.61
Ba_2AuSb[15]$^{\text{FP-LAPW}}$	98.362	196.214	160.39
Ba_2AuBi[15]$^{\text{FP-LAPW}}$	98.644	207.3	143.32

We observe that above the Fermi level, the conduction band is heavily dominated by Ba-4d and (As-4p^*, Sb-5p^*, Bi-6p^*) states for all R Heusler compounds, while below the Fermi level, in the top of the valence band represented by the three bands between 0 and -2 eV, TDOS is predominant by (As-4p, Sb-5p, Bi-6p) orbitals with a minor contribution from Ag-5s represented by the single valence band around -2.5 eV for Ba_2Ag(As, Sb, Bi) compounds, respectively. The two most electropositive atoms Ba donate their four $5s$ electrons to the electronegative Ag and (As, Sb, Bi) atoms. Thus, the Fully occupied $4d$ (represented by the flat valence bands around -4.5 eV) and $5s$ states of the Ag atom are extremely localized and far below the Fermi level, such that Ag only weakly interacts with its neighboring atoms. Also, the As-4s, Sb-5s, and Bi-6s electron lone pairs are deep below the Fermi level and are chemically inactive, represented by the single valence band around -9 eV. Therefore, as it is presented in Figs. (2-4)c, although the R compounds have in total ten valence electrons per f.u., these latter inactive (As-4s, Sb-5s, and Bi-6s) lone pairs lead effectively to an eight-electron system, resulting in filled bonding and empty antibonding states following the electron counting rule to obtain a semiconductor.

3.3. Thermodynamic properties

Thermodynamic properties of materials are closely related to their volume; therefore, examining the volume change under different working conditions of temperature and pressure is very important to design materials. Thermodynamic properties of the Ba_2AgZ (Z = As, Sb, Bi) R compounds have been determined using the GIBBS2 code, which is an implementation of the quasi-harmonic Debye model [24], in which the non-equilibrium Gibbs function $G^*(V;P,T)$ can be written in the next form:

$$G^*(V;P,T) = E(V) + PV + A_{vib}[\theta_D;T], \qquad (1)$$

where $E(V)$ is the total energy per unit cell, PV corresponds to the constant hydrostatic pressure condition, θ_D is the Debye temperature, and Avib is the vibrational term, which can be written using the Debye model of the phonon density of states as [25]:

$$A_{vib}[\theta_D;T] = nkT\left(\frac{9\theta}{8T} + 3\ln[1-e^{-\theta/T}] - D\left[\frac{\theta}{T}\right]\right), \qquad (2)$$

where n is the number of atoms per formula unit, $D(\theta/T)$ represents the Debye integral, and for anisotropic solid, θ is expressed as [25]:

$$\theta_D = \frac{h}{2\pi k}\left(6\pi^2V^2n\right)^{1/3} f(\sigma)\sqrt{\frac{B_s}{M}}, \qquad (3)$$

where M is the molecular mass per unit cell and B_S the adiabatic bulk modulus, approximated by the static compressibility [26]:

$$B_s \cong B(V) = V\frac{d^2E(V)}{dV^2}, \qquad (4)$$

where $f(\sigma)$ is given by Ref. [26]; σ is the Poisson ratio. Therefore, the non-equilibrium Gibbs function $G*(V;P,T)$ as the function of $(V;P,T)$ can be minimized with respect to volume V,

$$\left(\frac{\partial G^*(V;P,T)}{\partial V}\right)_{P,T} = 0. \qquad (5)$$

By solving Eq. (18), one can obtain the thermal equation of state (EOS) $V(P,T)$. The heat capacity C_V and the thermal expansion coefficient α are given by [27],

$$C_v = 3nk\left(4D\left[\frac{\theta}{T}\right] - \frac{3\theta/T}{e^{\theta/T}-1}\right), \qquad (6)$$

$$S = nk\left(4D\left[\frac{\theta}{T}\right] - 3\ln(1-e^{-\theta/T})\right), \qquad (7)$$

$$\alpha = \frac{\gamma C_V}{B_T V}. \qquad (8)$$

where γ is the Grüneisen parameter.

In this work, properties are calculated in a wide range of temperature and pressure, from 0 to 1000 K and from 0 to 20 GPa, respectively. Heat capacity C_V is related to the lattice vibrations and internal energy, which are responsible for

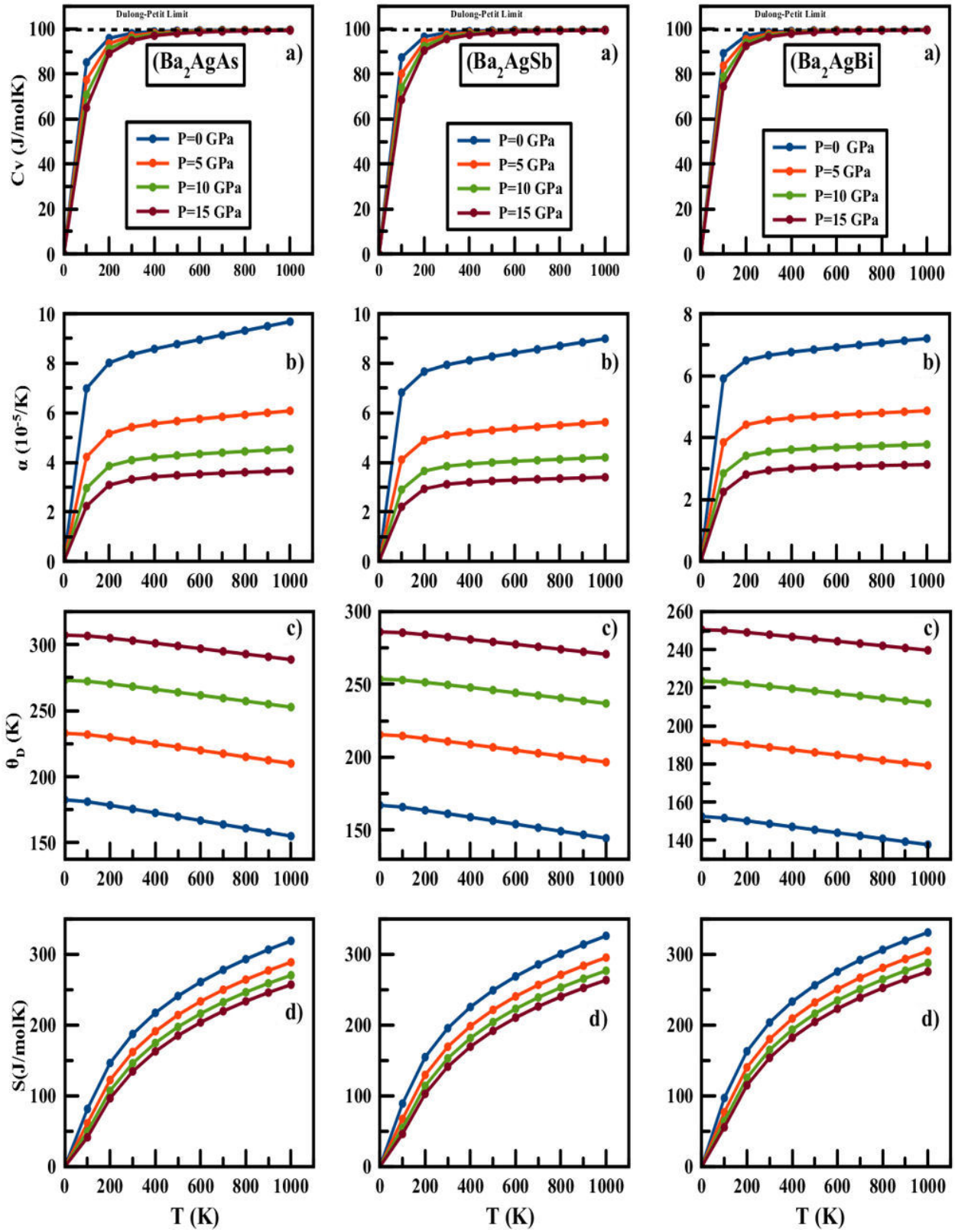

FIGURE 5. a) Heat capacity C_V, b) thermal expansion coefficient α, c) Debye temperature θ_D, and d) entropy S vs temperature and pressure for Ba_2AgZ (Z = As, Sb, Bi) alloys calculated by quasiharmonic Debye approximation.

many physical properties of materials. The variation of Ba_2AgZ (Z = As, Sb, Bi) heat capacity C_V as a function of temperature at fixed pressures is displayed in Fig. 5a). It is important to mention that at temperature 0 K, the heat capacity always takes zero value, implying the absence of lattice vibrations in the material.

The C_V, along with the temperature of all compounds, increases rapidly up to 200 K. Beyond this temperature, the rising rate decreases considerably, and the heat capacity tends to the saturation value, corresponding to the Dulong-Petit limit, indicating the thermal excitation of all phonon modes in all ours R compound. Results suggest that the lattice vibrations will become stronger by increasing temperature, and a contrary behavior can be obtained when raising pressure. A stronger dependence on temperature of the heat capacity is obtained than on pressure. The predicted values of specific heat of Ba_2AgAs, Ba_2AgSb, and Ba_2AgBi alloys at 300 K and 0 GPa are 98.08, 98.35, and 98.56 J·mol^{-1}·K^{-1}, respectively. Another important thermodynamic parameter for both theoretical study and practical design of materials is the thermal expansion coefficient α. In Fig. 5b), the Ba_2AgZ (Z = As, Sb, Bi) thermal expansion coefficient is depicted as a function of temperature at various pressures. We see that α increases as T^3 at low temperature, and above 200 K, an exponential increase is seen. Also, α decreases as the pressure increases where variation is more significant in the case of Ba_2AgAs as compared with Ba_2AgSb and Ba2AgBi.

Debye temperature is another thermodynamic parameter, which can be used to characterize the strength of covalent bonds. High values of Debye temperature also suggests the good hardness of the material, while low values are frequently found in soft materials. Figure 5c) shows the change of the Debye temperature under the effect of temperature (at several constant pressures). From these plots, it is found that the θ_D decreases with temperature in all ours compounds at different pressures. The variation suggests the effect of the anharmonic behavior of the solids. The calculated value of the Debye temperature θ_D at zero pressure and 300 K is found to be equal to 175.55, 161.26, and 148.61 K for Ba_2AgAs, Ba_2AgSb, and Ba_2AgBi, respectively, suggesting that Ba_2AgAs is harder than Ba_2AgSb and Ba_2AgBi. We have used the variation of entropy (S) to infer the nature of order and disorder, regarded as the main thermodynamic properties of a crystal. It is noticed from Fig. 5d) that at fixed pressures P, entropy S increases monotonously with the temperature T. The current investigations demonstrated that the lattice entropy behaves with strong pressure and temperature dependence, at 0 GPa and 300 K, S= 185.35, 195.68 and 203.73 J·mol^{-1}·K^{-1}, respectively.

3.4. Thermoelectric properties

In order to estimate the thermoelectric performance of ours compounds, we have computed the transport properties such as Seebeck coefficient S, thermopower factor PF, electrical conductivity σ, electronic thermal conductivity κ_e, and figure of merit ZT using the semiclassical Boltzmann theory and rigid band approach with accurate Brillouin zone (BZ) sampling with a dense grid of 100000 k-points to obtain convergence [28].

The transport coefficients σ, κ, S, ZT and PF as a function of temperature (T) and chemical potential (μ) are obtained from the following equations:

$$\sigma = \frac{1}{\Omega}\int \Xi_{i,k}\left(\frac{\partial f_0(T,\varepsilon)}{\partial \varepsilon}\right)d\varepsilon, \tag{9}$$

$$k_e = \frac{1}{T\sigma}k_B^2 T\int \Xi_{i,k}\left(\frac{\varepsilon-\mu}{k_B T}\right)^2\left(-\frac{\partial f_0(T,\varepsilon)}{\partial \varepsilon}\right)d\varepsilon, \tag{10}$$

$$S = \frac{e}{T\sigma}\int \Xi_{i,k}\left(-\frac{\partial f_0(T,\varepsilon)}{\partial \varepsilon}\right)(\varepsilon-\mu)d\varepsilon, \tag{11}$$

$$ZT = \frac{\sigma S^2 T}{k}, \tag{12}$$

$$PF = \sigma S^2, \tag{13}$$

where Ω is the volume of the unit cell and f_0 is the Fermi-Dirac distribution function, and $\Xi_{i,k}$ is the transport distribution kernel defined elsewhere [29].

The results are plotted in Fig. 6(a-f). An efficient thermoelectric material is required to have high electrical conductivity, low thermal conductivity, and a large Seebeck coefficient. The variation of the electrical conductivity σ/τ as a function of the temperature is plotted in Fig. 6a). The electrical conductivity (σ/τ) increases slowly up to 500 K and then after it increases sharply and at 1000 K attains a value of 2.33, 2, and 1.95 (10·19 Ω^{-1}·m^{-1}·s^{-1}) for Ba_2AgAs, Ba_2AgSb, and Ba_2AgBi, respectively. This behavior indicates the semiconducting nature of ours compound and thus supports the band structure.

Figures 6(b-d) displays the temperature dependences of total thermal conductivity ($\kappa_{tot} = \kappa_e + \kappa_L$), the lattice thermal conductivity κ_L, and the electronic thermal conductivity κ_e contributions. The lattice thermal conductivity was determined using Slack's equation [30]:

$$K_L = \frac{A\theta_D V^{1/3} M}{\gamma^2 n^{2/3} T}, \tag{14}$$

where θ_D is the Debye temperature, γ is the Grüneisen parameter, V is the volume per atom, n is the number of atoms in the primitive unit cell, M is the average mass of the atoms in the crystal, and T is an absolute temperature. The constant A is defined as:

$$A(\gamma) = \frac{5.72\times 0.847\times 10^7}{2\left(1-\left[\frac{0.514}{\gamma}\right]+\left[\frac{0.228}{\gamma^2}\right]\right)}. \tag{15}$$

It is clear that the temperature dependence of the electronic thermal conductivity κ_e is similar to the behavior of electrical conductivity. The lattice thermal conductivity decreased as the temperature increased in all materials because, at high temperatures, the phonon scattering is dominated by Umklapp processes and may stand it as a potential candidate

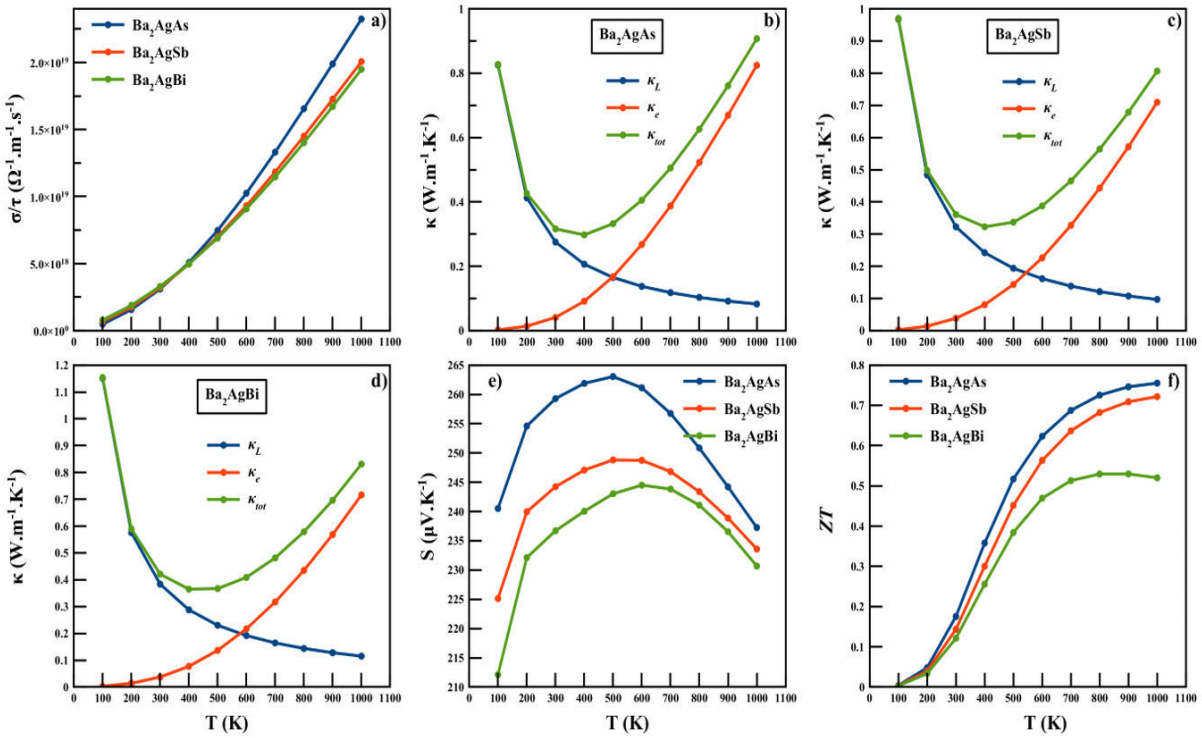

FIGURE 6. The variation of electrical conductivity σ/τ a), electronic thermal conductivity κ_e, lattice thermal conductivity κ_L, total thermal conductivity κ_{tot} b)-d), Seebeck coefficient S e) and figure of merit ZT f) as a function of temperature for Ba_2AgZ (Z = As, Sb, Bi) alloys.

for thermoelectrics. All ours R Heusler compound exhibit extremely low κ_L of 0.275, 0.323 and 0.384 W.m^{-1}·K^{-1} at 300 K for Ba_2AgAs, Ba_2AgSb, and Ba_2AgBi, respectively. The discovery of such low values of κ_L is all the more exciting since only complex crystal structures with large unit cells, *e.g.*, skutterudites and clathrates, which are well known for their low thermal conductivities where guest atoms rattle in the host cage structures and scatter the heat-carrying phonons [31,32]. Analogously to clathrates, the Ag atoms rattling are in a pseudocage structure composed of the alkali and main group atoms (Z). The strongly localized Ba-6s state leads to weak interactions with the 6p states of the Z-site atoms, such that Ag behaves like the inert alkaline (earth) metals in clathrate cages. So, in strong contrast to the common perception that only complex or host-guest structures with large unit cells can lead to such low thermal conductivity, R. Heusler compounds demonstrate that ultralow thermal conductivity can be realized in very simple crystal structures.

We have estimated the electrical conductivity as shown in Fig. 6a). As the temperature increases, an exponentially increasing trend can be seen, which may trigger its thermoelectric efficiency. This increasing conductivity is attributed to the semiconducting behavior of the alloys.

The variation of total thermal conductivity κ is shown in Figs. 6b)-d), where the electronic thermal conductivity κ_e increases with temperature, while the lattice part κ_L decreases with an increase in temperature. In the case of electronic thermal conductivity κ_e, as the temperature increases from 300 to 1000 K, the exponential increase occurs from 0.041, 0.0382, and 0.0373 W/mK to 0.825, 0.71, and 0.72 W/mK for Ba_2AgAs, Ba_2AgSb and Ba_2AgBi, respectively. In the case of lattice thermal conductivity κ_L, there is a decrease from 0.83, 0.97 and 1.15 W/mK at 100 K to 0.0825, 0.097, and 0.16 W/m Kat 1000 K for Ba_2AgAs, Ba_2AgSb, and Ba_2AgBi, respectively. These values are very small as compared to traditional Full Heusler alloys [6,10,13]. The capability of showing lower lattice thermal conductivity may stand it as a potential candidate for thermoelectrics.

The total thermal conductivity κ_{tot} shows an exponential decaying trend in all compounds up to 400 K due to the abrupt increase of large phonon vibrations before increasing slightly with temperature. We also computed the total Seebeck coefficient S variation calculated to designate its nature as shown in Fig. 6e). As one can see, the Seebeck coefficient of our R. Heusler compound is positive. The positive sign of S explains that the holes are dominant charge carriers. Therefore, our R. Heusler compounds are p-type materials. The calculated transport coefficients are now used to estimate the thermoelectric efficiency through the figure of merit ZT measurement. The materials are considered as good elements for thermoelectric devices if their ZT is about or greater than unity [33]. The variation of ZT is shown in Fig. 6f), which shows linearly that ZT increase with increasing temperature. At room temperature, these values are respectively 0.175, 0.143 and 0.121 for Ba_2AgAs, Ba_2AgSb and Ba_2AgBi. At 1000 K, its respective maximum values are 0.76, 0.73 and 0.52 respectively. It is clear that a higher temperature results in a higher figure of merit for the compound

TABLE IV. Values of electrical conductivity σ/τ (in 1018 $\Omega^{-1}\cdot m^{-1}\cdot s^{-1}$), lattice thermal conductivity κ_L ($W\cdot m^{-1}\cdot K^{-1}$), total thermal conductivity κ_{tot}(in $W\cdot m^{-1}\cdot K^{-1}$) and Seebeck coefficient S (in $\mu V\cdot K^{-1}$) and figure of merit ZT at 300 K for Ba_2AgZ (Z= As, Sb, Bi) and other Rattling [14-16] and Full Heusler compounds [6-10,13].

Compound	σ/τ	κ_L	κ_{tot}	S	ZT
Ba_2AgAs	3.1	0.275	0.316	260	0.1
Ba_2AgSb	3.2	0.323	0.361	244	0.143
Ba_2AgBi	3.3	0.384	0.421	237	0.121
Ba_2AuSb[15]				$1106.23^{\text{FP-LAPW}}$	
Ba_2AuBi		0.5[14]$^{\text{PAWF}}$		848.30[15]$^{\text{FP-LAPW}}$	
Ba_2HgPb[14]		0.5[14]$^{\text{PAWF}}$			
Sr_2PtSe[16]			$7.9^{\text{FP-LAPW}}$	$21.7^{\text{FP-LAPW}}$	$2.08\times10^{-3^{\text{FP-LAPW}}}$
Sr_2PtTe[16]			$8.7^{\text{FP-LAPW}}$	$9.02^{\text{FP-LAPW}}$	$1.27\times10^{-3^{\text{FP-LAPW}}}$
Li_2ZnGe[6]		$2.37^{\text{FP-LAPW}}$	$2.65^{\text{FP-LAPW}}$	$\sim -60^{\text{FP-LAPW}}$	$0.025^{\text{FP-LAPW}}$
Zr_2NiAl[7]	$3.0206^{\text{FP-LAPW}}$			$\sim -25^{\text{FP-LAPW}}$	$\sim 0.055^{\text{FP-LAPW}}$
Zr_2NiGa[7]	$2.1607^{\text{FP-LAPW}}$			$\sim -17.5^{\text{FP-LAPW}}$	$\sim 0.01^{\text{FP-LAPW}}$
Fe_2VAl		15[8]$^{\text{Exp}}$ 3.3[13]$^{\text{B1-WC}}$	16[8]$^{\text{Exp}}$ 28[10]$^{\text{Exp}}$	~ -20[8]$^{\text{Exp}}$	
Ru_2VAl[9]			$\sim 10^{\text{Exp}}$	$\sim -12.5^{\text{Exp}}$	$\sim 0.35\times10^{-3\text{Exp}}$
Ru_2VGa[9]			$\sim 13.5^{\text{Exp}}$	$\sim 8^{\text{Exp}}$	$\sim 0.6\times10^{-3\text{Exp}}$

TABLE V. Calculated thermoelectric power factors PF ($mW\cdot m^{-1}\cdot K^{-2}$) and corresponding optimal doping levels (carrier/unit cell) for p- and n-type doping at 300 K for Ba_2AgZ (Z= As, Sb, Bi) and other Rattling [14] and Full Heusler [13] compounds.

Compound	$p-$type doping level	PF	$n-$type doping level	PF
Ba_2AgAs	-0,45	15	+0.35	6.1
Ba_2AgSb	-0.461	9.6	+0.34	6.5
Ba_2AgBi	-0.422	9.2	+0.265	6.8
Ba_2AuBi[14]$^{\text{PAWF}}$	~ -0.6	10	$\sim +0.4$	6
Sr_2AuBi[14]$^{\text{PAWF}}$	~ -0.55	$\sim$10.5	$\sim +0.375$	$\sim$15.5
Fe_2VAl[13]$^{\text{B1-WC}}$	~ -0.6	$\sim$7	$\sim +0.45$	$\sim$3

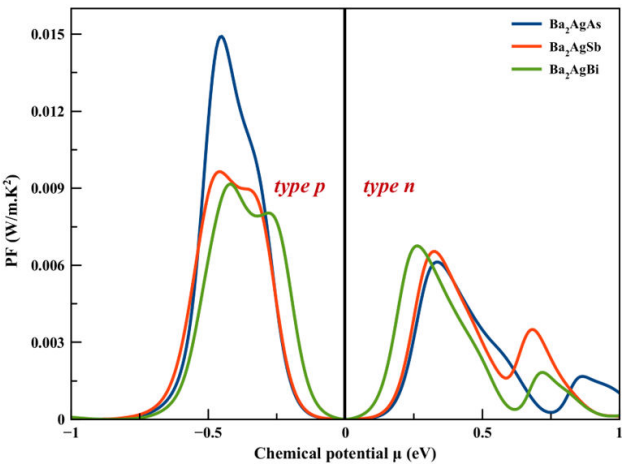

FIGURE 7. Power Factor (PF) of the Ba_2AgZ (Z = As, Sb, Bi) alloys at 300 K as a function of the chemical potential μ.

Ba_2AgAs with respect to Ba_2AgSb and Ba_2AgBi but Ba_2AgAs is regarded as a promising thermoelectric material. The value of electrical conductivity, thermal conductivity, Seebeck coefficient, and figure of merit ZT at room temperature are summarized in Table IV and compared with other R. Heusler [14-16] and Full Heusler compounds [6,7,9].

Finally, the applicability of material for thermoelectric technology is reflected in terms of power factor PF. The high power factor of material suggests high efficiency. The variation of power factor PF at 300 K as a function of chemical potentials (μ) are plotted in Fig. 7. The compound is considered pure at the zero chemical potential ($\mu = 0$ eV), which is located at the middle of the bandgap. The positive value of μ represents the n-type doping, while the negative μ describes the p-type doping. The optimal doping level at which the power factor reaches the highest value is one of the main aspects in the domain of thermoelectric compounds. From Fig. 7, it is clear that the PF of hole-doping (p-doping) is larger than that of electron-doping (n-doping); this signifies that p-type is better than n-type doping. Following the work of Bilc *et al.*, [13] and He *et al.* [14], a constant relaxation

time of $\tau = 3.4 \times 10^{-14}$ s was used. For p-type doping, an even larger PF of 15 m·W·m^{-1}·K^{-2} in Ba_2AgAs can be observed due to the "flat-and-dispersive" band at the L-point compared to both other R Heusler Ba_2AgSb and Ba_2AgBi. The maximum value of the power factor and the corresponding optimal doping levels for our alloys are presented in Table IV and compared with other R. Full Heusler [14] and F. Heusler [13] compounds.

4. Conclusion

Based on the density functional theory, we have employed the FP-LAPW method with the GGA approximation to investigate the structural, electronic, thermodynamic, and thermoelectric properties of the new Ba-based Rattling Full Heusler alloys Ba_2AgZ (Z = As, Sb, Bi). In all compounds, the stable $AlCu_2Mn$-type structure was energetically more favorable than the Hg_2CuTi-type structure. The calculated lattice constants and bulk modulus of the compounds are in good agreement with other theoretical data. From the study of the electronic properties, we predicted that these compounds have a semiconductor behavior with an indirect bandgap ($L - \Delta$). The quasi-harmonic Debye model was used to determine the thermodynamic properties comprising the thermal expansion, heat capacity, entropy, and Debye temperature parameter in the pressure range of $0 - 15$ GPa when the temperature varied from 0 to 1000 K. Boltzmann's theory was employed to study the thermoelectric properties which include electrical conductivity, electronic thermal conductivity, lattice thermal conductivity, Seebeck coefficient and power factor. These materials exhibit high values of Seebeck coefficient, and power factor and low lattice thermal conductivity with room temperature due to flat-and-dispersive valence bands. These properties establish these novel Rattling Full Heusler compounds as very promising thermoelectric materials. To our knowledge, no other studies of thermoelectric are available in the literature for these materials; thus, it would be beneficial to verify experimentally our predicted results.

Acknowledgments

This work has been supported by the PRFU project (N° B00L02UN220120190013) of the Ministry of Higher Education and Scientific Research (MESRS) and the Directory General of Scientific Research and Technological Development (DGRSTD).

1. E. Sasioglu, L.M. Sandratskii, P. Bruno, and I. Galanakis, Exchange interactions and temperature dependence of magnetization in half-metallic Heusler alloys, *Phys. Rev. B*, **72** (2005) 184415. https://doi.org/10.1103/PhysRevB.72.184415
2. H. Ishikawa, Y. Sutou, T. Omori, and K. Ishida, Pd-In-Fe shape memory alloy, *Appl. Phys. Lett.*, **90** (2007) 261906. https://doi.org/10.1063/1.2749440
3. B. Wiendlocha, M.J. Winiarski, M. Muras, C. Zvoriste-Walters, J.C. Griveau, S. Heathman, M. Gazda, and T. Klimczuk, Pressure effects on the superconductivity of the HfPd2Al Heusler compound: Experimental and theoretical study, *Phys. Rev. B*, **91** (2015) 024509. https://doi.org/10.1103/PhysRevB.91.024509
4. C. Felser, G. H. Fecher, and B. Balke, Spintronics: A Challenge for Materials Science and Solid-State Chemistry, *Angew. Chem. Int. Ed.* **46** (2007) 668. https://doi.org/10.1002/anie.200601815
5. C.S. Lue, J.W. Huang, D.S. Tsai, K.M. Sivakumar, and Y.K. Kuo, Effects of Ge substitution on the thermoelectric properties and pseudogap characteristics of Fe2VGa, *J. Phys.: Condens. Matter*, **20** (2008) 255233. https://doi.org/10.1088/0953-8984/20/25/255233
6. S. Yousuf, and D.C. Gupta, Ternary germanide Li2ZnGe: A new candidate for high temperature thermoelectrics, *J. Alloys Comp.*, **25** (2018), 501. https://doi.org/10.1016/j.jallcom.2017.12.211
7. S Yousuf, and D C Gupta, Investigation of electronic, magnetic and thermoelectric properties of Zr2NiZ (Z=Al,Ga) ferromagnets, *Mater. Chem. Phys.*, **192** (2017) 33e40
8. M. Mikami, Y. Kinemuchi, K. Ozaki, Y. Terazawa, and T. Takeuchi, Thermoelectric properties of tungsten-substituted Heusler Fe2VAl alloy, *J. Appl. Phys.*, **111** (2012) 093710. https://dx.doi.org/10.1063/1.4710990
9. B. Ramachandran, Y.H. Lin, Y.K. Kuo, C.N. Kuo, A.A. Gippius, and C.S. Lueb, Thermoelectric properties of Heusler-type $Ru_2VAl_{1-x}Ga_x$ alloys, *Intermetallics*, **92** (2018) 36. https://doi.org/10.1016/j.intermet.2017.09.012
10. Y. Nishino, S. Deguchi, and U. Mizutani, Thermal and transport properties of the Heusler-type $Fe_2VAl_{1-x}Ge_x$ ($0 \leq x \leq 0.20$) alloys: Effect of doping on lattice thermal conductivity, electrical resistivity, and Seebeck coefficient, *Phys. Rev. B*, **74** (2006) 115115. https://doi.org/10.1103/PhysRevB.74.115115
11. M. Vasundhara, V. Srinivas, and V.V. Rao, Electronic transport in Heusler-type $Fe_2VAl_{1-x}M_x$ alloys (M = B, In, Si), *Phys. Rev. B*, **77** (2008) 224415. https://doi.org/10.1103/PhysRevB.77.224415
12. E. J. Skoug, C. Zhou, Y. Pei, and D.T. Morelli, High Thermoelectric Power Factor Near Room Temperature in Full-Heusler Alloys, *J. Electron. Mater.*, **38** (2009) 1221. https://doi.org/10.1007/s11664-008-0626-x
13. D.I. Bilc, G. Hautier, D. Waroquiers, G.M. Rignanese, and P. Ghosez, Low-Dimensional Transport and Large Thermoelectric Power Factors in Bulk Semiconductors by Band Engineering of Highly Directional Electronic States, *Phys. Rev. Lett.*, **114** (2015) 136601. https://doi.org/10.1103/PhysRevLett.114.136601

14. J. He *et al*., Ultralow thermal conductivity in full Heusler semiconductors, *Phys. Rev. Lett.*, **117** (2016) 046602. https://doi.org/10.1103/PhysRevLett.117.046602
15. M. Matougui *et al*., Rattling Heusler Semiconductors Thermoelectric Properties: First-principles prediction, *Chinese J. Phys.* **57** (2018) 195. https://doi.org/10.1016/j.cjph.2018.11.015
16. M. Mana, F. Bendahma, and N. Benderdouche, Ab-initio investigation of optoelectronic and thermoelectric properties in new p-type Rattling Heuslers Sr2PtX (X= Se and Te), *Comput. Condens. Matter*, **25** (2020) e00497. https://doi.org/10.1016/j.cocom.2020.e00497
17. P. Hohenberg, and W. Kohn, Inhomogeneous Electron Gas, *Phys. Rev.*, **136** (1964) B864. https://doi.org/10.1103/PhysRev.136.B864
18. W. Kohn, and L.J. Sham, Self-Consistent Equations Including Exchange and Correlation Effects, *Phys. Rev. B*, **140** (1965) A1133. https://doi.org/10.1103/PhysRev.140.A1133
19. J.C. Slater, Energy Band Calculations by the Augmented Plane Wave Method, *Adv. Quantum Chem.*, **1** (1964) 35. https://doi.org/10.1016/S0065-3276(08)60374-3
20. P. Blaha, K. Schwartz, G.K.H. Madsen, D. Kvasnicka, and J. Liutz, WIEN2k An Augmented Plane Wave Plus Local OrbitalsProgram for calculating Cristal Properties (Vienna University of Technology, Vienna, Austria, 2001).
21. J. P. Perdew, S. Burke and M. Ernzerhof, Generalized Gradient Approximation Made Simple, *Phys. Rev. Lett.* **7** (1996) 3865. https://doi.org/10.1103/PhysRevLett.77.3865
22. S. Ouardi, G.H. Fecher, C. Felser, and J. Kubler, Realization of Spin Gapless Semiconductors: The Heusler Compound Mn2CoAl, *Phys. Rev. Lett.* **110** (2013) 100401. https://doi.org/10.1103/PhysRevLett.110.100401
23. X.T Wang *et al*., Electronic structures and magnetism of Rh3Z (Z=Al, Ga, In, Si, Ge, Sn, Pb, Sb) with DO_3 structures, *J. Magn. Magn. Mater.*, **378** (2015) 16. https://doi.org/10.1016/j.jmmm.2014.10.161
24. A. Otero-de-la-Roza, D. Abbasi-Pérez, and V. Luana, GIBBS2: A new version of the quasiharmonic model code. II. models for solid-state thermodynamics, features and implementation, *Comput. Phys. Commun.*, **182** (2011) 2232. https://doi.org/10.1016/j.cpc.2011.05.009
25. M.A. Blanco, A. Martín Pendás, E. Francisco, J.M. Recio, and R. Franco, Thermodynamical properties of solids from microscopic theory: applications to MgF2 and Al2O3, *J. Mol. Struct. Theochem.*, **368** (1996) 245. https://doi.org/10.1016/S0166-1280(96)90571-0
26. M. Florez, J.M. Recio, E. Francisco, M.A. Blanco, A. Martín Pendás, First-principles study of the rocksalt-cesium chloride relative phase stability in alkali halides, *Phys. Rev. B*, **66** (2002) 144112. https://doi.org/10.1103/PhysRevB.66.144112
27. R. Hill, The Elastic Behaviour of a Crystalline Aggregate, *Proc. Phys. Soc. London A* **65** (1952) 349. https://doi.org/10.1088/0370-1298/65/5/307
28. G. K. H. Madsen, and D. J. Singh, BoltzTraP. A code for calculating band-structure dependent quantities. *Comput. Phys. Commun.*, **175** (2006) 67. https://doi.org/10.1016/j.cpc.2006.03.007
29. T.M. Bhat and D.C. Gupta, Transport, Structural and Mechanical Properties of Quaternary FeVTiAl Alloy, *J. Electron. Mater.*, **45** (2016) 6012. https://doi.org/10.1007/s11664-016-4827-4
30. G.A. Slack, Nonmetallic crystals with high thermal conductivity, *J. Phys. Chem. Solids*, **34** (1973) 321. https://doi.org/10.1016/0022-3697(73)90092-9
31. J.S. Tse, Z. Li, and K. Uehara, Phonon band structures and resonant scattering in Na8Si46 and Cs8Sn44 clathrates, *Europhys. Lett.*, **56** (2001) 261. https://doi.org/10.1209/epl/i2001-00515-8
32. Y. He, and G. Galli, Nanostructured Clathrate Phonon Glasses: Beyond the Rattling Concept, *Nano Lett.*, **14** (2014) 2920. https://doi.org/10.1021/nl501021m
33. T. Takeuchi, *Mater. Trans.*, **50** (2009) 2359. https://doi.org/10.2320/matertrans.M2009143